

# Intercombination Effects in Resonant Energy Transfer

C L Vaillant,\* R M Potvliege, and M P A Jones†

*Department of Physics, Joint Quantum Centre (JQC) Durham-Newcastle,  
Durham University, South Road, Durham DH1 3LE, United Kingdom*

We investigate the effect of intercombination transitions in excitation hopping processes such as those found in Förster resonance energy transfer. Taking strontium Rydberg states as our model system, the breakdown of  $LS$ -coupling leads to weakly allowed transitions between Rydberg states of different spin quantum number. We show that the long-range interactions between two Rydberg atoms can be affected by these weakly allowed spin transitions, and the effect is greatest when there is a near-degeneracy between the initial state and a state with a different spin quantum number. We also consider a case of four atoms in a spin chain, and show that a spin impurity can resonantly hop along the chain. By engineering the many-body energy levels of the spin-chain, the breakdown of  $LS$  coupling due to inter-electronic effects in individual atoms can be mapped onto a spatial separation of the total spin and the total orbital angular momentum along the spin chain.

PACS numbers: 32.80.Ee, 34.20.Cf, 37.10.Jk, 87.15.Hj

The non-radiative exchange of energy due to dipole-dipole interactions plays a crucial role in biology, both in naturally occurring processes such as photosynthesis [1], but also as a tool for probing intra and inter-molecular distances [2]. The usual requirements for efficient energy transfer are an electric dipole-dipole interaction between donor and acceptor molecules, and a near degeneracy between the initial and final states that ensures the process is always resonant [2]. Resonant energy transfer has also been extensively studied in atomic physics, where these conditions are easily met. For example, dipole-dipole interactions in dense, optically excited samples can lead to cooperative Lamb shifts [3, 4]. By using Rydberg states, rather than low-lying electronic states, the strength of the interaction can be increased by many orders of magnitude, leading to energy exchange over macroscopic distances [5–12].

Resonant energy transfer is usually assumed to be mediated only by electric dipole interactions. Accordingly, it is usually assumed, in agreement with the dipole selection rules, that only states with the same value of the total electron spin quantum number  $S$  are coupled by these interactions. However, in atomic and molecular systems with more than one valence electron,  $S$  is at best an approximately good quantum number owing to inter-electronic interactions. Transitions between energy levels labelled as singlet and triplet therefore become weakly allowed, resulting in so-called intercombination lines. A canonical example is found in the group II elements such as Sr, where intercombination transitions are used as precision frequency standards [13, 14].

In this letter, we examine the impact of spin mixing on long-range interactions, considering first the effect of intercombination transitions on non-resonant van der Waals-type interactions, and second the effect of spin mixing on resonant hopping processes. As a model system we consider the  $5snd$  Rydberg states of strontium. Ultra-cold Rydberg gases of divalent atoms are of growing

interest in atomic physics [15–20], and as well as systems where the precise details of the electronic wave function are known [21–26], they provide a route to precise control of the inter-particle spacing via optical lattices or tweezer arrays [27–31]. Since strontium has two valence electrons, two Rydberg series with total angular momentum  $J = 2$  exist, one labelled as the singlet and one as a triplet. Early theoretical and experimental work showed that these energy eigenstates do not have a well defined spin due to their interaction with doubly excited “perturbors” of mixed singlet/triplet character [21, 22, 32]. These perturbors are coupled to the Rydberg states by inter-electronic interactions, resulting in a breakdown of  $LS$  coupling, which in turn affects the long-range inter-atomic interactions; the situation is depicted pictorially in Fig. 1(a). We find that, for two interacting strontium atoms, the  $2 \times n$   $^3D_2$  states are close in energy to the  $(n-2)$   $^1F_3 + (n-3)$   $^3F_3$  states near  $n = 30$  (as shown in Fig. 1(b)), which, combined with the spin-mixing in the Rydberg series, allows near-resonant transfer between two-atom states. For the case of four atoms, we find that a spin impurity (a  $28$   $^1F_3$  atom) in a chain of  $30$   $^3D_2$  atoms can hop resonantly from site to site, showing a spin-forbidden propagation along the chain (as shown in Fig. 1(c)).

Although here we consider only specific cases, we anticipate that similar effects may be important elsewhere, given the ubiquity of spin mixing effects and the increased probability of degeneracy in molecular systems with broad energy bands. Important examples could include Förster coupled quantum dots, where intercombination effects have previously been considered [33], and excitonic energy transfer in organic light emitting devices [34].

We begin by considering two atoms in  $5snd$   $^3D_2$  states. Theoretically, this situation is most easily treated using multi-channel quantum defect theory, which provides a wave function for each single-atom energy eigenstate in

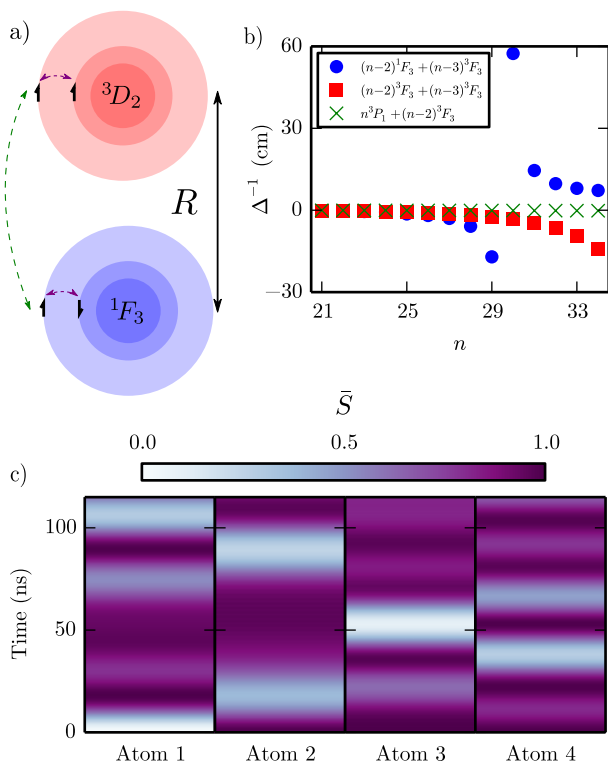


FIG. 1. (color online) (a) Two Rydberg atoms separated by a distance  $R$  are prepared in different spin states. Interactions between core and valence electrons (purple dashed arrow) leads to a breakdown of  $LS$  coupling, enabling an otherwise forbidden dipole-dipole interaction to take place (green dashed arrow). (b) The inverse of the energy separation between the  $2 \times 30$   ${}^3D_2$  pair states and the energetically closest spin allowed (red squares, green crosses) and spin forbidden (blue circles) final pair states, showing a spin-forbidden resonance. (c) Spin-forbidden propagation of a singlet spin impurity ( $28$   ${}^1F_3$ , initially located at Atom 1) along a short chain of triplet ( $30$   ${}^3D_2$ ) Rydberg atoms, with a spacing of  $a = 2.0$   $\mu\text{m}$  between the atoms. Shading indicates the mean spin quantum number  $\bar{S}$  at each site as a function of time.

terms of a superposition of  $LS$ -coupled channels. Recently, we carried out an improved MQDT analysis of these states based on up-to-date experimental results, which gave the amount and nature of each electronic state (singlet, triplet perturber) present in each of the  $J = 2$  energy eigenstates [21]. We use these wave functions to examine the long-range interaction between a pair of atoms prepared in the same  $5snd$   ${}^3D_2$  energy eigenstate. Each of these pair states is coupled by electric dipole transitions to other final pair states (e.g.  $P + P$ ,  $P + F$ ,  $F + F$ ). Because of spin mixing, the final states may or may not differ in  $S$  from the initial state. A key parameter is the energy difference between the final state and the initial state — the so-called Förster defect — which must be compared to the strength of the coupling. Fig. 1(b) shows an example where a near-degeneracy occurs in the spin-forbidden channel, i.e. where the spin labels of

the initial and final states are different. Thus, although the spin mixing, and hence the coupling, is weak, this spin-forbidden process can become important.

More concretely, to describe the long-range interactions, we consider each atomic energy eigenstate,  $\Psi$ , to be a sum over the MQDT channel states,  $\phi_k$ , such that  $\Psi = \sum_k \bar{A}_k \phi_k \chi_k$  (where  $\chi_k$  is a function describing the angular, spin and remnant core state wave functions [21]). Using these state vectors, the long-range interactions can be calculated either perturbatively (which corresponds to calculating a  $C_6$  coefficient [35]; details of the calculation are supplied in the supplementary material) or non-perturbatively (by diagonalizing an effective Hamiltonian matrix in a basis of pair states [35]). The values of the coefficients  $\bar{A}_k$ , as well as numerical dipole matrix elements, are provided in [21]. Throughout this paper, we only consider atoms that are initially in the stretched state ( $J = |M_J|$ ), with the internuclear axes of the interacting atoms being aligned with the  $z$ -axis. Stretched states do not have any degeneracies in  $M_{J_1} + M_{J_2}$ , thereby reducing the number of states that need to be considered (even allowing for the fact that the dipole-dipole interaction couples stretched states to non-stretched states).

The results of the  $C_6$  calculations (where the dipole-dipole interaction is given by  $C_6 R^{-6}$ ) are shown in Fig. 2, along with the contribution from “spin-allowed” (i.e. singlet-singlet, triplet-triplet) and “spin-forbidden” (singlet-triplet) intermediate pair states. Large contributions from singlet-triplet pair states are found in both series around  $n = 16$  where the effect of the  $4d6s$   ${}^1D_2$  and  ${}^3D_2$  perturbers is at its maximum [22, 35]. The overall  $C_6$  coefficients for states in this region differ significantly from predictions based on single-channel quantum defect calculations for Rydberg states below  $n = 30$ . Above  $n = 30$ , however, all effects from perturbers are found to contribute less than 2% of the overall  $C_6$ , thus validating the use of a one-electron treatment for high-lying Rydberg states of strontium [26, 35, 36].

Also visible in Fig. 2 is a large singlet-triplet contribution for  ${}^3D_2$  states close to  $n = 30$ . This arises due to the Förster resonance in the  $2 \times n {}^3D_2 \rightarrow (n-2) {}^1F_3 + (n-3) {}^3F_3$  channel shown in Fig. 1(b). The uncertainties in the energy levels used to calculate the  $C_6$  coefficients [35] are large enough that the location of the Förster resonance can change by one value of  $n$ , however the resonance is always present to within the error of these energy level measurements [22, 35, 37]. The small Förster defect in this channel means that second-order perturbation theory is no longer valid, and we turn to a non-perturbative calculation. Fig. 3 shows the non-perturbative Born-Oppenheimer potential curves in the vicinity of the  $30$   ${}^3D_2 + 30$   ${}^3D_2$  asymptote, which has a spin-forbidden avoided crossing at relatively large distances with the  $28$   ${}^1F_3 + 27$   ${}^3F_3$  asymptotic pair state. Without the mixing between the triplet and singlet se-

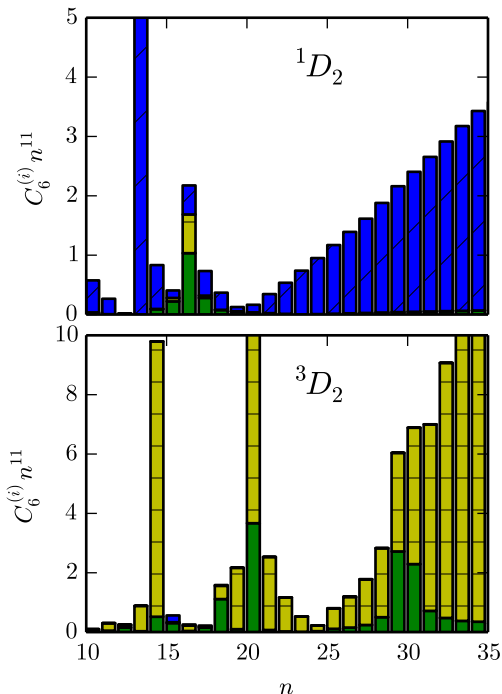


FIG. 2. (color online) Absolute value of the contributions to the  $C_6$  coefficients (with the dominant  $n^{11}$  scaling factored out for clarity) from the singlet-singlet (blue diagonally-lined bars), singlet-triplet (green) and triplet-triplet (red horizontally-lined bars) pair states acting as intermediate states. The initial states are taken to be in their stretched state, with  $J = M_J$ .

ries, the avoided crossing would not exist. Because of the small defect, the interaction between these pair states is stronger than could be expected in view of the smallness of the singlet-triplet mixing in these Rydberg states.

As another illustration of the impact of this intercombination Förster resonance on resonant energy transfer, we now examine the propagation of a singlet “impurity” in a short chain of four equally spaced atoms. Denoting the  $30\ ^3D_2$ ,  $28\ ^1F_3$ ,  $27\ ^3F_3$ , and  $28\ ^3F_3$  states by  $|0\rangle$ ,  $|1\rangle$ ,  $|2\rangle$ , and  $|3\rangle$ , respectively, we numerically calculate the time evolution of the system at time  $t$  after the  $|1000\rangle$  state is prepared. Restricting the dynamics of each atom to these four states is justified by the fact that the  $C_6$  coefficient of the  $2 \times 30\ ^3D_2$  is dominated by the Förster-resonant  $28\ ^1F_3 + 27\ ^3F_3$  and the non-resonant  $28\ ^3F_3 + 27\ ^3F_3$  pair states. All other pair states contribute less than 15% to the  $C_6$  coefficient of the  $2 \times 30\ ^3D_2$  state and are far enough away in energy to be neglected. Fig. 3 shows the consequence of only choosing the four single atom states,  $30\ ^3D_2$ ,  $28\ ^3F_3$ ,  $27\ ^3F_3$ , and  $28\ ^1F_3$ ; the potential curve for the  $30\ ^3D_2 + 30\ ^3D_2$  asymptote is shown to be well reproduced. We include all values of  $M_J$  that contribute.

Fig. 1(c) shows the evolution of the average value of

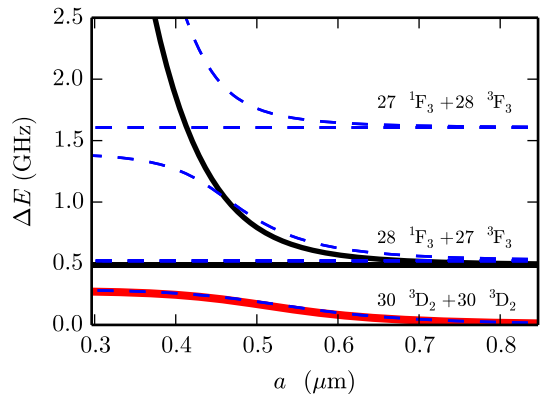


FIG. 3. (color online) Dipole-dipole potential curves for two atoms around the state labelled  $30\ ^3D_2 + 30\ ^3D_2$  at infinity. The blue dashed curves represent the full non-perturbative calculation including all the relevant pair states, and the solid curves show the results of the four-level approximation (the red curve highlights the initial state,  $2 \times 30\ ^3D_2$ ). Only the  $M_{J_1} = M_{J_2} = 2$  states are shown for the  $30\ ^3D_2 + 30\ ^3D_2$  state.

the spin quantum number,  $\bar{S}_p = \sum_i S_p^{(i)} |c^{(i)}(a, t)|^2$  for a lattice spacing of  $2\ \mu\text{m}$  (a spacing that can be engineered using two crossed 1550 nm laser beams [19, 38]). Here  $p$  refers to the lattice site, the index  $i$  runs over all the  $4^4$  uncoupled 4-atom states  $|q_1 q_2 q_3 q_4\rangle$  ( $q_p = 0, \dots, 3, p = 1, \dots, 4$ ),  $S_p^{(i)}$  is the spin quantum number of the atomic state  $q_p$  in the uncoupled 4-atom state  $i$ , and  $c^{(i)}(a, t)$  is the amplitude of this uncoupled 4-atom state in the state of the dipole-coupled chain at time  $t$ . The spin can be seen to propagate along the chain of atoms and back, although there is additional state transfer due to competing second-order interactions. The calculation shown in Fig. 1(c) includes the interactions between all the atoms, not just nearest-neighbour interactions. Nevertheless, a clear propagation of a spin singlet state through the chain can be seen, a phenomenon that can only occur due to spin-mixing.

For the parameters of Fig. 1(c), the dynamics arise primarily from the spin-forbidden dipole-dipole coupling between the  $|1000\rangle$ ,  $|0100\rangle$ ,  $|0010\rangle$  and  $|0001\rangle$  states. The spin-forbidden Förster resonance between the  $|00\rangle$  and  $|12\rangle$  or  $|21\rangle$  pair states also has an impact on the dynamics of this spin chain. For instance, the potential energy curves shown in Fig. 4(a) (red lines) exhibit an avoided crossing between states of predominantly  $|1000\rangle$  and  $|1120\rangle$  character (these states are linear combinations of several unperturbed states due to the interactions). As a result, the average value of the total angular momentum quantum number at each site,  $\bar{J}_p = \sum_i J_p^{(i)} |c^{(i)}(a, t)|^2$ , may vary differently with  $t$  and  $p$  than the average value of the spin quantum number,  $\bar{S}_p$ , as shown in Fig. 4(b)-(d). The key feature is that, due to the interactions, the

inter-electronic effects responsible for the breakdown of  $LS$  coupling *within* each atom are now manifested spatially in the *collective* state of the spin chain. Moving from  $a = 2 \mu\text{m}$  to  $a = 1.3 \mu\text{m}$  would reduce the energy gap between the  $|1120\rangle$  and  $|1000\rangle$  families, further increasing the significance of this effect.

Alternatively, an external field can be used to enhance the impact of the  $|1\rangle$  and  $|2\rangle$  states on the dynamics of the chain, without reducing the lattice spacing. We have found that static electric fields do not provide the required tunability and a very large magnetic field (730 G) would be required to completely cancel the Förster defect (see supplementary material). However, the desired result can be obtained by applying an off-resonant circularly polarized microwave field to AC Stark shift the  $30 \ ^3D_2$  state upwards. The microwave field is detuned from the  $30 \ ^3D_2 \rightarrow 30 \ ^1P_1$  transition which has frequency  $\omega_0 = 34 \text{ GHz}$ . The detuning is assumed to be small, such that the other Rydberg states shift much less than the  $30 \ ^3D_2$  state. As the  $F$  states are not dipole-coupled to the  $30 \ ^1P_1$  states, the  $30 \ ^3D_2$  state is the only state of interest to be significantly affected by the light shift. With a detuning  $\Delta = 460 \text{ MHz}$  and Rabi frequency  $\Omega = 20.6 \text{ MHz}$ , we obtain an AC Stark shift of 230 MHz which fully cancels the Förster defect, with an admixture of 0.1% of the  $30 \ ^1P_1$  level. Fully cancelling the Förster defect, however, is unnecessary to observe the separation in the dynamics between the average spin and angular momentum. A light shift of 165 MHz causes the energy levels to be nearly degenerate at infinite lattice spacing, meaning that the energy separation at  $a = 2.0 \mu\text{m}$  between the  $|1000\rangle$  and  $|1120\rangle$  states is entirely due to the dipole-dipole interactions, implying strong state mixing, as shown in Fig. 4(d). In contrast, for the microwave-free case the energy levels are far apart and the state mixing is localized around the avoided crossing, resulting in very little state mixing at  $a = 2.0 \mu\text{m}$ , as is the case in Fig. 4(c).

We turn to the feasibility of observing this effect in a lattice of ultra-cold strontium atoms. The first issue that must be considered is the finite lifetime of the Rydberg states concerned, which we obtain using MQDT. The natural lifetimes of the  $30 \ ^3D_2$  and  $28 \ ^1F_3$  states are  $2.3 \mu\text{s}$  and  $6.9 \mu\text{s}$  respectively [21, 39], which are much longer than the time scales of the dynamics of the spin chain. The triplet  $F$  state lifetimes are unknown, but can be expected to be similar in magnitude to the  $30 \ ^3D_2$  and  $28 \ ^1F_3$  states. The required lattice spacings are larger than the state-of-the-art Rydberg lattices that have already been demonstrated [40, 41], making the preparation of these spin chains feasible with current technology. In order to image the dynamics, short microwave pulses could be used to state-selectively transfer the population to other Rydberg states that do not interact resonantly, thus “freezing” the dynamics. Spatial resolution could then be obtained by using spatially and

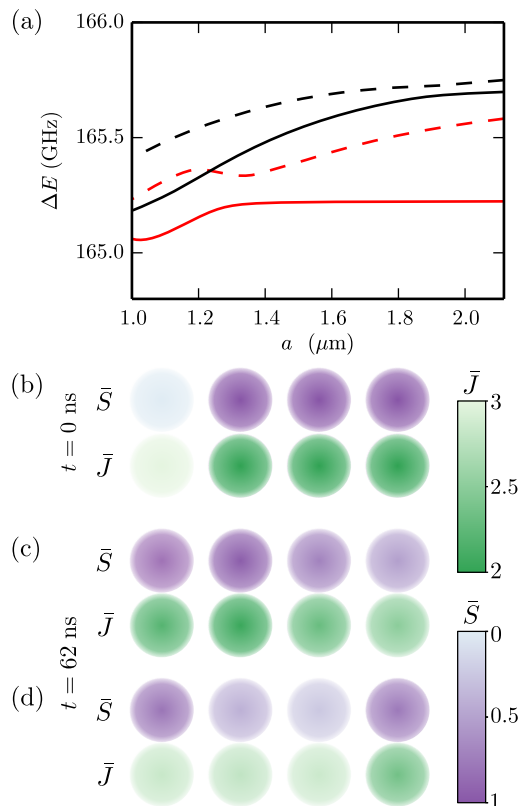


FIG. 4. (color online) (a) Energy of the  $|1000\rangle$  state (solid lines) and the  $|1120\rangle$  state (dashed lines) for a spin chain of four atoms equally separated by a distance  $a$  from their nearest neighbours. Black lines: results with the microwave field acting, giving a light shift of 165 MHz. Red lines: results without a microwave field. Sub-figures (b) to (d) show the average values of the quantum numbers (as defined in the main text) for the spin chain with  $a = 2.0 \mu\text{m}$ . (b) Spin chain for  $t = 0 \text{ ns}$ . (c) Spin chain without the microwave field, at  $t = 62 \text{ ns}$ . (d) Spin chain with the microwave field, also at  $t = 62 \text{ ns}$ .

spectroscopically resolved fluorescence detection.

In conclusion, we have shown that intercombination transitions in Sr Rydberg atoms not only lead to a breakdown of  $LS$  coupling but also allow dipole-forbidden excitation hopping along a chain of atoms via resonant long-range dipole-dipole interactions. Until now, these  $S$ -changing transitions have been considered negligible, which we show to mostly be the case for very high values of the principal quantum number  $n$ . Even at high  $n$ , though, we find that intercombination Förster resonances can have a substantial impact on the long-range interactions. The intercombination Förster resonance also gives rise to a collective breakdown of  $LS$  coupling in a spin chain, leading to spatially separated dynamics between the average spin and total angular momentum quantum numbers. Although we use Sr Rydberg states as an example, we expect that other systems with singlet-triplet mixing may show similar effects.

The authors would like to thank S A Gardiner and C W Weiss for useful discussions. Financial support was provided by EPSRC grant EP/J007021/1 and EU grant FP7-ICT-2013-612862-HAIRS. The data used in this publication can be freely downloaded from <http://dx.doi.org/10.15128/cc24b379-1be2-4c42-862b-9760aa257077>.

---

\* c.l.j.vaillant@durham.ac.uk

† m.p.a.jones@durham.ac.uk

- [1] Y.-C. Cheng and G. R. Fleming, *Annu. Rev. Phys. Chem.* **60**, 241 (2009).
- [2] G. D. Scholes, *Annu. Rev. Phys. Chem.* **54**, 57 (2003).
- [3] J. Keaveney, A. Sargsyan, U. Krohn, I. G. Hughes, D. Sarkisyan, and C. S. Adams, *Phys. Rev. Lett.* **108**, 173601 (2012).
- [4] R. Röhlsberger, K. Schlage, B. Sahoo, S. Couet, and R. Rüffer, *Science* **328**, 1248 (2010).
- [5] D. Barredo, H. Labuhn, S. Ravets, T. Lahaye, A. Browaeys, and C. S. Adams, *Phys. Rev. Lett.* **114**, 113002 (2015).
- [6] T. Vogt, M. Viteau, A. Chotia, J. Zhao, D. Comparat, and P. Pillet, *Phys. Rev. Lett.* **99**, 073002 (2007).
- [7] I. I. Ryabtsev, D. B. Tretyakov, I. I. Beterov, and V. M. Entin, *Phys. Rev. Lett.* **104**, 073003 (2010).
- [8] T. Vogt, M. Viteau, J. Zhao, A. Chotia, D. Comparat, and P. Pillet, *Phys. Rev. Lett.* **97**, 083003 (2006).
- [9] C. S. E. van Ditzhuijzen, A. F. Koenderink, J. V. Hernández, F. Robicheaux, L. D. Noordam, and H. B. van Linden van den Heuvell, *Phys. Rev. Lett.* **100**, 243201 (2008).
- [10] G. Günter, H. Schempp, M. Robert-de Saint-Vincent, V. Gavryusev, S. Helmrich, C. S. Hofmann, S. Whitlock, and M. Weidemüller, *Science* **342**, 954 (2013).
- [11] W. R. Anderson, J. R. Veale, and T. F. Gallagher, *Phys. Rev. Lett.* **80**, 249 (1998).
- [12] I. Mourachko, D. Comparat, F. de Tomasi, A. Fioretti, P. Nosbaum, V. M. Akulin, and P. Pillet, *Phys. Rev. Lett.* **80**, 253 (1998).
- [13] A. Derevianko and H. Katori, *Rev. Mod. Phys.* **83**, 331 (2011).
- [14] B. J. Bloom, T. L. Nicholson, J. Williams, S. L. Campbell, M. Bishof, X. Zhang, W. Zhang, S. L. Bromley, and J. Ye, *Nature* **506**, 71 (2014).
- [15] J. Millen, G. Lochead, and M. P. A. Jones, *Phys. Rev. Lett.* **105**, 213004 (2010).
- [16] L. I. R. Gil, R. Mukherjee, E. M. Bridge, M. P. A. Jones, and T. Pohl, *Phys. Rev. Lett.* **112**, 103601 (2014).
- [17] S. Ye, X. Zhang, T. C. Killian, F. B. Dunning, M. Hiller, S. Yoshida, S. Nagele, and J. Burgdörfer, *Phys. Rev. A* **88**, 043430 (2013).
- [18] P. McQuillen, X. Zhang, T. Strickler, F. B. Dunning, and T. C. Killian, *Phys. Rev. A* **87**, 013407 (2013).
- [19] R. Mukherjee, J. Millen, M. P. A. Jones, and T. Pohl, *J. Phys. B* **44**, 184010 (2011).
- [20] G. Lochead, D. Boddy, D. P. Sadler, C. S. Adams, and M. P. A. Jones, *Phys. Rev. A* **87**, 053409 (2013).
- [21] C. L. Vaillant, M. P. A. Jones, and R. M. Potvliege, *J. Phys. B* **47**, 155001 (2014).
- [22] P. Esherick, *Phys. Rev. A* **15**, 1920 (1977).
- [23] M. Aymar, E. Luc-Koenig, and S. Watanabe, *J. Phys. B* **20**, 4325 (1987).
- [24] M. Hiller, S. Yoshida, J. Burgdörfer, S. Ye, X. Zhang, and F. B. Dunning, *Phys. Rev. A* **89**, 023426 (2014).
- [25] T. Topcu and A. Derevianko, *Phys. Rev. A* **89**, 023411 (2014).
- [26] J. Millen, G. Lochead, G. R. Corbett, R. M. Potvliege, and M. P. A. Jones, *J. Phys. B* **44**, 184001 (2011).
- [27] V. D. Ovsiannikov, A. Derevianko, and K. Gibble, *Phys. Rev. Lett.* **107**, 093003 (2011).
- [28] T. Ido and H. Katori, *Phys. Rev. Lett.* **91**, 053001 (2003).
- [29] F. Nogrette, H. Labuhn, S. Ravets, D. Barredo, L. Béguin, A. Vernier, T. Lahaye, and A. Browaeys, *Phys. Rev. X* **4**, 021034 (2014).
- [30] M. J. Piotrowicz, M. Lichtman, K. Maller, G. Li, S. Zhang, L. Isenhower, and M. Saffman, *Phys. Rev. A* **88**, 013420 (2013).
- [31] M. Schlosser, S. Tichelmann, J. Kruse, and G. Birkel, *Quantum Inf. Process.* **10**, 907 (2011).
- [32] J. J. Wynne, J. A. Armstrong, and P. Esherick, *Phys. Rev. Lett.* **39**, 1520 (1977).
- [33] A. O. Govorov, *Phys. Rev. B* **71**, 155323 (2005).
- [34] M. A. Baldo, D. F. O'Brien, Y. You, A. Shoustikov, S. Sibley, M. E. Thompson, and S. R. Forrest, *Nature* **395**, 151 (1998).
- [35] C. L. Vaillant, M. P. A. Jones, and R. M. Potvliege, *J. Phys. B* **45**, 135004 (2012).
- [36] M. C. Zhi, C. J. Dai, and S. B. Li, *Chinese Phys.* **10**, 929 (2001).
- [37] J. R. Rubbmark and S. A. Borgström, *Phys. Scripta* **18**, 196 (1978).
- [38] K. D. Nelson, X. Li, and S. Weiss, *Nature Phys.* **3**, 556 (2007).
- [39] G. Jönsson, C. Levinson, A. Persson, and C.-G. Wahlström, *Z. Phys. A* **316**, 255 (1984).
- [40] S. E. Anderson, K. C. Younge, and G. Raithel, *Phys. Rev. Lett.* **107**, 263001 (2011).
- [41] C. Weitenberg, M. Endres, J. Sherson, M. Cheneau, P. Schauss, T. Fukuhara, I. Bloch, and S. Kuhr, *Nature* **471**, 319 (2011).